Direct sensor orientation based on GPS network solutions

Helge Wegmann[a], Christian Heipke[b], Karsten Jacobsen[b]

[a]Ingenieurbüro Wegmann,
Leo-Rosenblatt-Weg 6, 30453 Hannover, Germany
info@ib-wegmann.de

[b]Institute for Photogrammetry and GeoInformation, University of Hannover,
Nienburger Str. 1, 30167 Hannover, Germany
heipke, jacobsen@ipi.uni-hannover.de

Commission I, WG V

KEY WORDS: GPS, IMU, Direct image orientation

ABSTRACT:

Direct sensor orientation, i.e. the determination of exterior orientation based on GPS and inertial measurements without the need for photogrammetric tie points, has gained considerable popularity over the last years. One pre-condition for direct sensor orientation is a correct sensor and system calibration. The calibration can only be carried out by a combination of a photogrammetric solution and a GPS/inertial solution, which is equivalent to the concept of integrated sensor orientation.
In the work carried out so far, GPS has been identified as the most critical part in terms of achievable accuracy. Strategies for improving differential GPS results are available for terrestrial applications, but have not yet been used in direct and integrated sensor orientation. One of these solutions consists in using a network of reference stations rather than a single station only.
In this paper we present our work on direct sensor orientation using a GPS network. After describing the related mathematical models we report the results of an experimental test. The test data were drawn from the OEEPE test "Integrated sensor orientation". The results show, that while for many applications a network may not be necessary in case of short baselines and good GPS data, it still improves the accuracy of direct sensor orientation to some degree. More important is the fact, that our approach is able to detect gross errors in the reference station data and therefore has the potential to improve also the reliability of the results.

1 Introduction

The development of sensors and related processing methods for the economic, accurate and reliable collection of 3D geo-spatial information has been a topic of intense photogrammetric research in recent years. Besides the new digital aerial cameras, sensors for directly determining the exterior orientation based on GPS and inertial measurement units (IMU) have found large interest. The integration of GPS and the inertial measurement system has been strongly promoted at the University of Calgary for a long time already (Schwarz et al. 1984; 1993) and in the meantime a series of tests and pilot projects has been conducted demonstrating the potential of these methods (e.g. Skaloud 1999, Cramer 1999, Heipke et al. 2002b). The current situation is that GPS has been identified as the most critical part in terms of achievable accuracy.

When using GPS and IMU observations to determine the exterior orientation of photogrammetric images, one can differentiate between the so called *integrated sensor orientation*, in which all available information including tie points is processed simultaneously to achieve highest accuracy, and *direct sensor orientation*, in which the exterior orientation is computed based on GPS/IMU observations only, and object space coordinates are derived in a separate step (Heipke et al, 2002a).

Direct sensor orientation consists of three steps - a sensor calibration step to be carried in advance, as well as GPS/IMU pre-processing and the determination of the exterior orientation for the actual mission.
During sensor calibration the parameters describing each sensor individually and those describing the relationship between the different sensors need to be determined. These parameters include the interior orientation of the camera, the angular differences between the IMU and the image coordinate system (boresight misalignment), and additional parameters modelling e.g. GPS errors. The system calibration parameters, and in particular the boresight misalignment, can only be determined by comparing a photogrammetric solution based on image coordinates of ground control and tie points with the pre-processed GPS/IMU results.
GPS/IMU pre-processing includes the transformation of the raw GPS signal and IMU measurements into trajectories in object space for the camera projection centres and roll, pitch and yaw values at a high frequency (usually 50 – 200 Hz). The common method of integrating GPS and IMU observations is via Kalman filtering. It provides the optimum estimation of the system based on all past and present information (for details see Grewal et al. 2001).
The determination of the exterior orientation parameters then consists in applying the sensor calibration to the pre-processed GPS/IMU values. One of the applications of direct sensor orientation is 3D point determination via spatial forward intersection based on the refined exterior orientation parameters.

In this paper, we deal with direct sensor orientation and present as a novel aspect of our work a GPS network solution for photogrammetric point determination. In the next section we describe our model for sensor calibration based on pre-processed GPS/IMU data. We do not deal with GPS/IMU pre-processing itself. We then introduce our test data which are drawn from the OEEPE test "Integrated Sensor Orientation". We derive sensor calibration parameters, and compute 3D coordinates of independent check points which we compare to the known values, both with single reference stations, and using the GPS network. Finally, we comment our results and draw some conclusions for future work.

2 Mathematical model for integrated sensor orientation

For sensor calibration a common model of all three groups of observations (image coordinates of tie and ground control points (GCP), pre-processed data for the projection centre coordinates, pre-processed data for the angles of exterior orientation) needs to be set up. This model is the same as used in integrated sensor orientation, where all available information is processed simultaneously in order to obtain the highest accuracy. In this section, the model is outlined in some degree of detail. We finally turn to the description of the GPS network solution.

2.1 Model for image coordinates

The *image coordinates* are connected to the object space coordinate system via the well-known collinearity equations. The collinearity equations are based on an orthonormal coordinate system. Obviously, the national coordinate systems (e.g. UTM) do not correspond to this requirement. In traditional photogrammetry the effects of non-orthogonality are sometimes compensated by an earth curvature correction applied to the image coordinates. For a combined adjustment with image coordinates and direct observations of position and attitude this approach is not sufficient, because also the attitude observations need to be corrected, and different scale factors must be introduced for planimetry and height (see e.g. Jacobsen 2002; Ressl 2002). A more straightforward way is to transform all object space information into an orthonormal system a priori, e.g. a local tangential system. In the following we use such a local tangential system. Where necessary, this system is denoted by the symbol *m*.

The system of non-linear observation equations reads

$$\begin{aligned} x' + v_{x'} &= x'_o - f * \frac{r_{11}(X - Xo) + r_{21}(Y - Yo) + r_{31}(Z - Zo)}{r_{13}(X - Xo) + r_{23}(Y - Yo) + r_{33}(Z - Zo)} + dx' \\ y' + v_{y'} &= y'_o - f * \frac{r_{12}(X - Xo) + r_{22}(Y - Yo) + r_{32}(Z - Zo)}{r_{13}(X - Xo) + r_{23}(Y - Yo) + r_{33}(Z - Zo)} + dy' \end{aligned} \quad (1)$$

x', y', $v_{x'}$, $v_{y'}$	image coordinates and related residuals
X,Y,Z	object space coordinates for tie points and GCP
Xo,Yo,Zo	object space coordinates of projection centre
r_{ik}	elements of rotation matrix R^m_i (ω,φ,κ) between the image coordinate system and the object space coordinate system
x'_o, y'_o	image coordinates of the principal point
dx',dy'	corrections of the image coordinates
f	calibrated focal length

In order to introduce stochastic properties for the coordinates of the GCP, they are introduced as unknowns into the adjustment, and direct observations for the control point coordinates are set up within the model.

2.2 Position equations

The second part of the integrated sensor orientation model deals with the *pre-processed observations for the position of the projection centre*. These observations are often given in some Earth-fixed reference system, e.g. WGS 84, and need to be transformed into the local tangential system prior to using them in integrated sensor orientation. The model is extended by bias and drift parameters to describe linear systematic effects of position, as is sometimes also done in GPS-supported aerial triangulation (Jacobsen 1991; Ackermann 1994). An additional parameter dt takes care of a possible time synchronisation offset between the instant of image exposure and the GPS/IMU time.

$$\begin{pmatrix} \underline{X}_{GPS/IMU} \\ \underline{Y}_{GPS/IMU} \\ \underline{Z}_{GPS/IMU} \end{pmatrix}(t) + \begin{pmatrix} v_{X_{GPS/IMU}} \\ v_{Y_{GPS/IMU}} \\ v_{Z_{GPS/IMU}} \end{pmatrix} = \begin{pmatrix} X_O \\ Y_O \\ Z_O \end{pmatrix}(t+dt) + \quad (2)$$

$$R^m_i(t+dt)(\omega,\rho,\kappa)\begin{pmatrix} dx^{GPS/IMU}_{camera} \\ dy^{GPS/IMU}_{camera} \\ dz^{GPS/IMU}_{camera} \end{pmatrix} + \begin{pmatrix} b\_Xo \\ b\_Yo \\ b\_Zo \end{pmatrix} + (t+dt-to)\begin{pmatrix} d\_Xo \\ d\_Yo \\ d\_Zo \end{pmatrix}$$

$X,Y,Z_{(GPS/IMU)}$	object space coordinates of IMU centre of
$v_X,v_Y,v_{Z(GPS/IMU)}$	mass and related residuals
t	observation time of GPS/IMU
dt	synchronisation offset between GPS/IMU time and instant of camera exposure
t_o	reference epoch for drift computation
Xo,Yo,Zo	object space coordinates of projection centre, time dependent
$R^m_i(\omega, \varphi,\kappa)$	rotation matrix between the image coordinate system and the object space coordinate system, time dependent
$dx,dy,dz^{GPS/IMU}_{camera}$	components of offset vector between IMU centre and projection centre, expressed in image coordinate system
b_XoYoZo	bias in position (one parameter per strip, or one for the whole block)
d_XoYoZo	drift in position (one parameter per strip, or one for the whole block)

2.3 Attitude equations

The third part of the model describes the *pre-processed attitude observations*. In principle, these observations describe the rotation between the IMU coordinate system (so called body system *b*) and an inertial coordinate system. In strap down navigation, the inertial system is replaced by a local level system, the so called navigation system *n* (see e. g. Bäumker, Heimes 2002). The x-axis of the navigation system points northwards, the z-axis downwards along the local plumb line, the y-axis completes the right-handed system. Besides other corrections, the transformation from inertial to navigation system requires the knowledge of Earth rotation and gravity parameters, and is usually integrated into GPS/IMU pre-processing.
Thus, the pre-processed attitude observations describe the rotation of *b* around *n*. In aerial applications, the body system is fixed to the aircraft. *b* and the related rotation angles roll, pitch, and yaw are defined according to the aviation norm ARINC 705 (ARINC 2001).

Since the IMU measurements refer to the local plumb line, the navigation system is not an Earth-fixed system, but moves together with the IMU. A connection to the photogrammetric rotations is given via the Earth fixed system *e*. The instantaneous position of the aircraft is expressed in

geographic coordinates (λ_i, ϕ_i) taken from the GPS/IMU positions. A rotation can then be set up from *n* to *e*, another one to the local tangential system *m* centred at the geographic coordinates (λ_o, ϕ_o) and used in the collinearity equations. Additional rotations need to be introduced to take into account the different axes direction of the navigation and the local tangential system on the one hand, and the body and the image coordinate system on the other hand. Finally, the misalignment between the image coordinate system and the body system must be included. Since the misalignment is considered as constant, it must be expressed in the body system rather than in the image coordinate system. As in the case of the position equations the system is completed by bias and drift parameters.

The non-linear observation equations for attitude are given by

$$\begin{pmatrix} roll \\ pitch \\ yaw \end{pmatrix}^n_b (t) + \begin{pmatrix} v_{roll} \\ v_{pitch} \\ v_{yaw} \end{pmatrix} = T\,[R^n_e(\lambda_i,\varphi_i)\cdot R^e_{n_0}(\lambda_o,\varphi_o)\cdot R^{n_0}_m(\pi,0,-\frac{\pi}{2})$$

$$\cdot R^m_i(t+dt)(\omega,\phi,\kappa)\cdot R^i_{b^*}(\pi,0,0)\cdot R^{b^*}_b(\Delta roll,\Delta pitch,\Delta yaw)\,] \qquad (3)$$

$$+\begin{pmatrix} b\_roll \\ b\_pitch \\ b\_yaw \end{pmatrix}^n_b + (t+dt-to)\begin{pmatrix} d\_roll \\ d\_pitch \\ d\_yaw \end{pmatrix}^n_b$$

$(roll, pitch, yaw)^n_b$	elements of rotation matrix between *b*
$v_{roll}, v_{pitch}, v_{yaw}$	and *n* and related residuals
T	function to extract a vector of rotation angles out of the rotation matrix
ω,φ,κ	angles of exterior orientation, time dependent
λ_i, ϕ_i	geographic coordinates of IMU at the instant of exposure
λ_o, ϕ_o	geographic coordinates of origin of local tangential system
Δroll, Δpitch, Δyaw	angles of boresight misalignment
R^n_e	rotation matrix between Earth-fixed and navigation system
R^e_{no}	rotation matrix between navigation system at the origin of the local tangential system and Earth-fixed frame
R^{no}_m	rotation matrix between local tangential system and fixed navigation system
R^m_i	rotation matrix between image coordinate system and local tangential system
$R_{b^*}{}^i$	rotation matrix between body system altered by misalignment and image coordinate system
$R_b{}^{b^*}$	rotation matrix of boresight misalignment
b_roll, pitch, yaw	bias in attitude (one parameter per strip or one or the whole block)
d_roll, pitch, yaw	drift in attitude (one parameter per strip or one or the whole block)
t, dt, t_o	see above

2.4 Least-squares adjustment

Equations (1) to (3) form the mathematical model of integrated sensor orientation, which is also used to determine the system calibration parameters necessary for direct sensor orientation, as mentioned above. Different sets of calibration parameters can be chosen. Besides the boresight misalignment, the bias parameters of equation (2) are often selected as calibration parameters. Depending on the available data and the intended use of the calibration results, also the interior orientation parameters of the camera, and the synchronisation offset dt can be considered as unknowns.

Of course, it must be ensured that the selected parameters can be computed in a numerically stable way from the provided information. For instance, assuming a flat test field a correction to the calibrated focal length and a bias parameter in Z can only be determined if imagery from at least two different flying heights is available, and a correction to the principal point in flight direction together with a bias in flight direction requires at least two strips flown in opposite directions. Also, the synchronisation offset dt is highly correlated with the correction for the principal point in flight direction, a separation needs again two different flying heights. Finally, in order to interpolate the corrected exterior orientation parameters at the instant of image exposure after having estimated dt at the end of each adjustment iteration, high resolution information for position and attitude must be available.

The unknowns of the approach are computed in a least-squares adjustment, based on the principle

$$v^T P v \text{ -> minimum} \qquad (4)$$

As usual, P is the weight matrix of the observations. It should be noted that often no stochastic information is available for the GPS/IMU measurements after the Kalman filtering if commercial software is used for GPS/IMU pre-processing.

2.5 GPS network solution

We now address the GPS network solution. It is well known, that the observation quality in differential GPS depends on the length of the baseline (Seeber 2003). In other applications GPS network solutions, i.e. solutions involving more than one reference station, have found major interest and are increasingly also used in practical applications. In photogrammetry, such possibilities have not yet been exploited.

Based on the described formulae, we can create a network solution in two different ways: first, we can consider each available reference station individually and set up equations (2) and (3) for each image as often as there are reference stations. An alternative is to combine the observations of the different reference stations during GPS/IMU pre-processing, and to subsequently set up equations (2) and (3) only once per image. The first possibility has the advantage of simplicity, since pre-processing can be done in the conventional way. The second possibility has the advantage of being able to analyse in detail the different high frequency GPS/IMU observations, and to eliminate any error at an early stage. Also, different sets of calibration parameters can be taken into account for the different reference stations. Since at present we do not have the possibility to do GPS/IMU pre-processing, we have decided to use this first possibility for our studies.

The characteristics of the network solution are as follows:

(1) if there are multiple baselines of similar length, the different reference stations have the effect of repeated measurements.
(2) if the baselines are different in length, and thus the quality of the GPS/IMU observations differs, the network solution yields an average result, which is obviously not as accurate as the one for the shortest baseline, but better than the one for the longest baseline.
(3) if there are short term errors in any of the baselines, the network solution is able to reduce, and perhaps to eliminate, the effect of these errors.

In any case, multiple baselines lead to a larger redundancy of the adjustment system, and thus to an increased possibility for detecting gross errors, and to a more reliable solution for the parameters of exterior orientation. Of course, any problems connected to the GPS receiver in the aircraft cannot be detected, neither can the standard deviation of computed object space coordinates be improved, if the limiting factor is the measurement accuracy of the corresponding image coordinates, and not the exterior orientation.

3 Test data

In order to analyse our model we used the data of the OEEPE test "Integrated sensor orientation" (see Heipke et al. 2002a; b and Nilsen 2002). For this paper we used only a subset of the test data.
The test was flown over the test field Fredrikstad in Southern Norway. The test field has a size of approximately 4,5*6 km^2 and contains about 50 signalised GCP with object space coordinates known to sub-centimetre accuracy.
The aircraft was flown at an altitude of 1.600 meters above ground resulting in an image scale of approximately 1:10.000. Two flights were selected: the calibration flight included four strips, two strips in west-east and east-west direction and two further strips in north-south and south-north direction; and a project flight with five strips in north-south and south-north direction. In order to achieve a good initial alignment for the IMU axes with the gravity field, the aircraft made an S-like turn before the first flight strip. Image coordinates of a sufficient number of tie points and of all GCP were measured manually on an analytical plotter.
The selected GPS/IMU aircraft equipment was a POS/AV 510-DG from Applanix, consisting of a high quality off-the-shelf navigation grade IMU as typically used in precise airborne position and attitude determination. The POS/DG equipment was tightly coupled to a wide angle Leica RC30, the latter mounted on the gyro-stabilised platform PAV30. The PAV30 data and thus rotations of the camera and the IMU relative to the plane body were recorded at 200 Hz and introduced into further processing. The claimed accuracy is better than 0.1 m for the IMU position, and better than 0.005 degree in roll and pitch, and better than 0.008 degree in yaw (Applanix 1999).
During data acquisition several GPS reference stations were used and the GPS equipment in the aircraft and on the reference stations consisted of dual frequency receivers performing differential carrier phase measurements at 2 Hz.

The following reference stations were used for the results reported in this paper:

- Raade (baseline 8 – 30 km),
- Moss (baseline 15 – 38 km),
- Torp (20-50 km baseline),
- Soer (25-60 km baseline),
- Stavanger (baseline approx. 307 km).

The different values for the baselines are caused by the flight pattern, for Stavanger this effect amounts to only 10 % of the length and is negligible. Figure 1 shows the accuracy of the GPS-position for the reference station Raade for the various strips of the project flight. In the upper part of the figure, the PDOP (position dilution of precision), a common descriptor for GPS position accuracy (Seeber 2003) can be seen as the straight line, the baseline length is the more undulated line. It is clearly visible that the PDOP increases sharply during the first strip indicating some problem in the GPS signal, and only decreases after the fourth strip. In the lower part, the resulting GPS accuracies in X, Y, and Z derived from processing different satellites (but no IMU data) are shown. The correlation between the large PDOP value and the large standard deviations for the GPS position can clearly be seen.

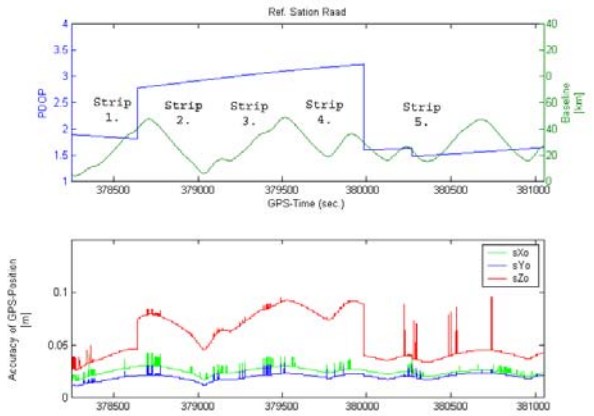

Figure 1: Accuracy of GPS position, reference station Raade

The small peaks in the X,Y and Z accuracies in the lower part of figure 1 can be smoothed when introducing IMU data during Kalman filtering. It is not possible, however, to compensate the weaker accuracy over the longer time period in the same way. Only a network solution or additional GCP can overcome this problem.

4 Sensor calibration

Based on the model explained in section 2 and the calibration flight data described in section 3 we performed a calibration of the equipment used in the test. The displacement vector between the GPS antenna and the IMU centre of mass was determined before the flight mission using conventional surveying techniques and was used as a constant lever arm correction.

Since we only had one flying height, we selected the six standard parameters (boresight misalignment and GPS offset parameters). In addition, we solved for a time synchronisation offset. In the adjustment, we introduced twelve GCP, together with sufficient, well distributed image coordinates of tie points together with the pre-processed position and attitude data. Initial values for all unknowns could also be made available.

The standard deviations used for the weight matrix were as follows (see table 1):

image coordinates	± 6 µm
object space coords. of GCP	± 0.01 m in X,Y and Z
GPS/IMU position	± 0.1 m
GPS/IMU roll, pitch	± 5 deg * 10^{-3}
GPS/IMU yaw	± 8 deg * 10^{-3}

Table 1: Standard deviations of observations used for sensor calibration

All observations were considered as uncorrelated, because no other information was available. The values for the position and attitude data are those reported by Applanix.

In the adjustment, all seven parameters could be determined with high significance. Whereas the results for the six conventional parameters were relatively small, the time offset was found to be 5.3 msec with standard deviation of 0.3 msec, and thus approximately one cycle of the 200 Hz data set. As mentioned before, however, this value must be interpreted as a combination of time offset and correction to the principal point in flight direction.

5 3D point determination

5.1 Point determination with a single baseline

In the next step, we computed object space coordinates for those GCP which had not been used in the calibration. We used the images from the project flight and only two rays per point and computed the 3D coordinates via forward intersection. In this step the calibration parameters were used as constant values[1]. The project flight was covered by approximately 50 stereo models. All computations were carried out for each of the available five reference stations.

The results are shown in table 2. For each baseline the mean accuracy of the GPS/IMU observations are given. The position values come from differential GPS solutions and represent more or less the accuracy of the GPS geometric configuration (satellite visibility and length of baseline). The attitude values had to be taken from the company information since no other information was available. In the right column the RMS differences between the computed object space coordinates and the known values for the 41 independent control points (most of them were not introduced in the calibration phase) are given.

The results are in the range of 8 cm in planimetry and 15 cm in height at independent check points for short baseline (until 60 km). For the longer baseline at Stavanger (approximately 300 km) we obtained RMS values in the range of 10 cm in X, Y and 19 cm in Z. The differences represent the weaker geometric GPS configuration and possibly different atmospheric conditions between the test field and Stavanger, which can not be compensated by differential GPS strategies. It should be mentioned that these results, obtained with imagery of scale 1:10.000 compare very favourable to the results obtained in the OEEPE test (Heipke et al. 2002b).

[1] Note that separate sets of calibration parameters were computed for each reference station, and these were used in all following computations.

Ref. station (length of baseline)	**Mean accuracy of GPS/IMU position and attitude**				**RMS differences at ICP [cm]**	
	position [cm]		**attitude [deg * 10^{-3}]**			
	Xo Yo	**Zo**	**roll, pitch**	**yaw**	**X,Y**	**Z**
Raade (8-30 km)	2,5	6,7	~ 5	~ 8	8,0	14,5
Moss (15-38 km)	3,1	7,1	~ 5	~ 8	8,1	14,8
Torp (20-50 km)	3,5	8,2	~ 5	~ 8	8,3	15,1
Soer (25-60 km)	3,5	8,1	~ 5	~ 8	8,5	15,4
Stavanger (307 km)	4,5	11,5	~ 5	~ 8	10,2	19,1

Table 2: Results of direct 3D point determination at independent check points (ICP) using two-ray points and single reference stations, image scale 1:10.000

5.2 GPS network solution

We now turn to the GPS network solution. In order to better demonstrate the effects of this approach we select only two strips, one with good overall GPS data, and another one with somewhat worse data.

Figure 2 shows the same information for the reference station Torp as figure 1 does for Raade. It can be seen that strip 1 has a small and thus a good PDOP value for both reference stations. Strip 2 has a small PDOP for Torp, but a higher one for Raade. The graphs for the reference stations Moss and Soer are similar to those for Raade.

We therefore expect, that the results of strip 1 will be good overall, and will not be effected by the network solution. Strip 2, on the other hand, should show good results when computed with station Torp, but worse results when computed from Raade. One of the questions was in how far a network solution would be able to improve the results obtained with the Raade station.

The results are shown in table 3. The expected tendency can be observed when inspecting the values in the table,

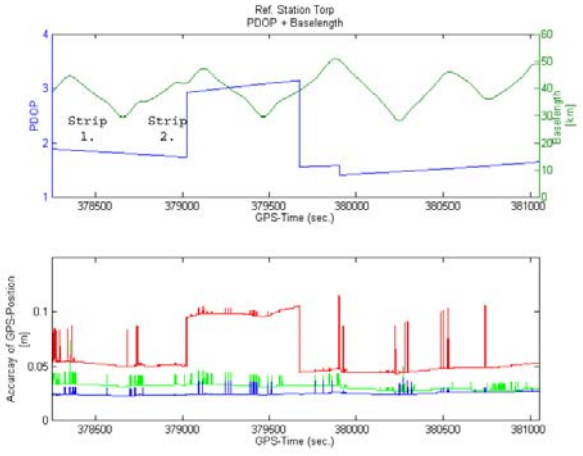

Figure 3: Accuracy of GPS position, reference station Torp

especially in height. The RMS values in Z of strip 2 for Raade, Moss and Soer are larger than the one for Torp. It can also be seen that the network solution yields slightly better results especially compared to those stations with a larger PDOP.

While the improvements in accuracy are not very large in this example, it should be kept in mind, that potential GPS errors occurring at a particular reference station cannot be detected if only one station is used. Therefore, the reliability of a solution based on a single reference station is not very high. By using the suggested network solution, which has already found wide applicability in other GPS applications, the reliability of the results can be significantly improved. Having said this, it should also be mentioned that problems concerning the GPS receiver in the aircraft can of course only be detected and eliminated by using multiple GPS equipment on board the plane.

Used ref. Station	**Strip**	**PDOP**	**RMS differences at ICPs (two-ray-points)**	
			sXY [cm]	**SZ [cm]**
Raade (8 – 30 km)	Strip 1	1,8	7,8	13,7
	Strip 2	3,3	8,3	14,8
Moss (15–38 km)	Strip 1	1,8	8,1	14,1
	Strip 2	3,2	8,4	14,5
Torp (20–50 km)	Strip 1	1,7	8,1	14,0
	Strip 2	1,9	7,9	13,9
Soer (35–60 km)	Strip 1	1,9	8,2	14,6
	Strip 2	3,3	8,9	15,8
Network solution (8 – 60 km)	Strip 1	-	7,9	13,8
Network solution (8 – 60 km)	Strip 2	-	8,0	14,0

Table 3: Results of direct 3D point determination at independent check points (ICP) using two-ray points and single reference stations and the network solution, individual strips, image scale 1:10.000

6 Conclusion

Direct sensor orientation has proven to be a serious alternative to aerial triangulation. In this paper, a solution for direct sensor orientation based on single reference stations and on a GPS network was described, test results based on the OEEPE test "Integrated sensor orientation" were reported.

Our work resulted in RMS differences of 8 cm in planimetry and 14 cm in height at independent check points obtained with two-ray points an image scale 1:10 000 for single, short baselines.

The network solution was shown to be slightly more accurate than the single baseline solution, moreover the reliability of the results is significantly higher.

7 References

Ackermann, F. 1994: *On the status and accuracy performance of GPS photogrammetry*. In: Proceedings, ASPRS Workshop "Mapping and remote sensing tools for the 21st Century, Washington D.C., USA, pp. 80-90.

Applanix 1999: POS/DG POS/AV 510-DG Specifications, http://www.applanix.com, Ontario, Canada (May 6, 2004).

ARINC 705 2001: http://www.arinc.com/cgi-bin/store/arinc (May 6, 2004).

Bäumker, M.; Heimes, F. J. 2002: *New Calibration and Computing Method for Direct Georeferencing of Image and Scanner Data Using the Position and Angular Data of an Hybrid Intertial Navigation System* in: Integrated Sensor Orientation, OEEPE Official Publication No. 43, Bundesamt für Kartographie und Geodäsie, Frankfurt/Main, pp. 197 – 212.

Cramer, M. 1999: *Direct geocoding - is aerial triangulation obsolete?* In: *Photogrammetric Week ´99*; Fritsch/Spiller (Ed.), Herbert Wichmann Verlag, Heidelberg, pp. 59 - 70.

Grewal, M. S.; Andrews A. P., 2001:*Kalman Filtering Theory and Practice Using Matlab*; Wiley-Interscience Publication, New York (USA). pp. 401.

Heipke, C.; Jacobsen, K.; Wegmann, H.; Andersen O.; Nilsen Jr. B. 2002 (a): *Test goals and test set up for the OEEPE test "Integrated Sensor Orientation"*. In: Integrated Sensor Orientation, OEEPE Official Publication No. 43, Bundesamt für Kartographie und Geodäsie, Frankfurt/Main, pp. 11 - 18.

Heipke, C.; Jacobsen, K.; Wegmann, H. 2002 (b): *Analysis of the results of the OEEPE test "Integrated Sensor Orientation"*. In: Integrated Sensor Orientation, OEEPE Official Publication No. 43, Bundesamt für Kartographie und Geodäsie, Frankfurt/Main, pp. 31 - 49.

Jacobsen, K. 1991: *Trends in GPD photogrammetry*, ASPRS Annual Convention 1991, Baltimore, Vol. 5, pp 208 – 217.

Jacobsen, K. 2002: *Transformations and computation of orientation data in different coordinate systems.* In: Integrated Sensor Orientation, OEEPE Official Publication No. 43, Bundesamt für Kartographie und Geodäsie, Frankfurt/Main, Germany, pp. 179-188.

Nilsen Jr., B. 2002: *Test field Frederikstad and data acquisition for the OEEPE test "Integrated Sensor Orientation"* in: Integrated Sensor Orientation, OEEPE Official Publication No. 43, Bundesamt für Kartographie und Geodäsie, Frankfurt/Main, Germany, pp. 19 - 30.

Ressl, C., 2002: *The impact of conformal map projections on direct georeferencing.* International Archives of Photogrammetry and Remote Sensing, Vol. 34, Part 3A, pp. 283-288. ISPRS Commission III Symposium 2002, Sept. 9-13, Graz, Austria.

Schwarz, K. P.; Fraser, C.; Gustafson, P. 1984: *Aerotriangulation without Ground Control*, International Archives of Photogrammetry and Remote Sensing, Vol. 25, Part A1, pp. 237-250.

Schwarz K.-P.; Chapman M.E.; Cannon E., Gong P. 1993: *An integrated INS/GPS approach to the georeferencing of remotely sensed data*, Photogrammetric Engineering & Remote Sensing Vol. 59, No. 11, pp. 1667-1674.

Seeber, G. 2003: *Satellite Geodesy 2nd Edition. Foundations, Methods and Applications*; Walter de Gruyter, Berlin.

Skaloud, J. 1999: *Optimizing Georeferencing of Airborne Survey Systems by INS/DGPS*. Ph. D. Thesis, UCGE Report 20216 University of Calgary, Alberta, Canada. pp. 160.